



The multiphysics analysis of the metallic bipolar plate by the electrochemical micro-machining fabrication process

Yu-Ming Lee^a, Shuo-Jen Lee^{a,*}, Chi-Yuan Lee^a, Dar-Yuan Chang^{b,1}

^a Department of Mechanical Engineering, Yuan Ze University, Yuan Ze Fuel Cell Center, 135 Yuan Tong Road, Chungli City, Taoyuan 320, Taiwan, ROC

^b Department of Mechanical Engineering, Chinese Culture University, 55, Hwa-Kang Road, Yang-Ming-Shan, Taipei, Taiwan, ROC

ARTICLE INFO

Article history:

Received 15 October 2008

Received in revised form 12 February 2009

Accepted 12 March 2009

Available online 31 March 2009

Keywords:

Bipolar plate

Electrochemical micro-machining (EMM)

Flow channel

Fabrication accuracy

Multiphysics model

ABSTRACT

In this study, the flow channels of a PEM fuel cell are fabricated by the EMM process. The parametric effects of the process are studied by both numerical simulation and experimental tests. For the numerical simulation, the multiphysics model, consisting of electrical field, convection, and diffusion phenomena is applied using COMSOL software. COMSOL software is used to predict the parametric effects of the channel fabrication accuracy such as pulse rate, pulse duty cycle, inter-electrode gap and electrolytic inflow velocity. The proper experimental parameters and the relationship between the parameters and the distribution of metal removal are established from the simulated results. The experimental fabrication tests showed that a shorter pulse rate and a higher pulse current improved the fabrication accuracy, and is consistent with the numerical simulation results. The proposed simulation model could be employed as a predictive tool to provide optimal parameters for better machining accuracy and process stability of the EMM process.

© 2009 Elsevier B.V. All rights reserved.

1. Introduction

A fuel cell is a power generator suitable for use in automobiles and electronic devices. A bipolar plate is an important component of the fuel cell and makes up most of the volume and weight of the fuel cell. Especially for graphite or composite material bipolar plates, due to their low mechanical properties, it is not easy to reduce the volume of these plates. Metallic materials such as stainless steel, aluminum, and titanium as an alternative material for bipolar plates are a rather recent research topic [1–3]. Metallic material has great mechanical properties but lacks machining processes for channel fabrication, especially in micro-scale channels.

The electrochemical micro-machining (EMM) process is an anodic dissolution process with electrochemical reaction. It is a zero-stress process suitable for any conducting material, especially super alloys. To fabricate a flow channel in a bipolar plate, the anode dissolves during the process, creating an inverse image of the cathode tool.

The electrical field or current is another key factor in EMM fabrication, especially when pulse current is being proposed to

improve the machining accuracy. Pulse current provides a micro-perturbation of the gas pressure which enhances the flow of the electrolyte, thereby improving the surface quality and the dimensional accuracy [4].

Bhattacharyya and Munda [5] demonstrated that a significant metal removal rate and minimal overcutting could be obtained with the proper operating potential, proper electrolytic concentration and sufficient processing time. Kock et al. [6] verified the effects of the pulse width on fabrication accuracy. Fabrication accuracy of 100 nm could be obtained with a 200 MHz repetition rate. Rosenkranz et al. [7] experimented with the pulse rate in order to improve the distribution of the electric current. He discussed the effects of the operating potential, pulse rate and distance of the electrode gap. A highly accurate 8 nm diameter and 20 nm deep hole was drilled in a SUS 304 stainless steel plate. Bhattacharyya et al. [8] proposed a low operating potential, sufficient electrolytic concentration and a high pulse rate to improve the amount of micro-sparkling and metal removal.

The above mentioned literatures all used a cathode electrode in the shape of a milling tool incorporated in the NC machining path. For a channel fabrication mechanism, it is much simpler than using the “forming” process used in this research. However, from a mass production point of view, the forming process may have better potential. The goal of this research is to establish a multiphysics model for a surface-shaped electrode in order to study the effects of the parameters and to improve the fabrication accuracy.

* Corresponding author. Tel.: +886 3 4637016; fax: +886 3 4558013.

E-mail address: mesjl@saturn.yzu.edu.tw (S.-J. Lee).

¹ Tel.: +886 2 2861 0511.

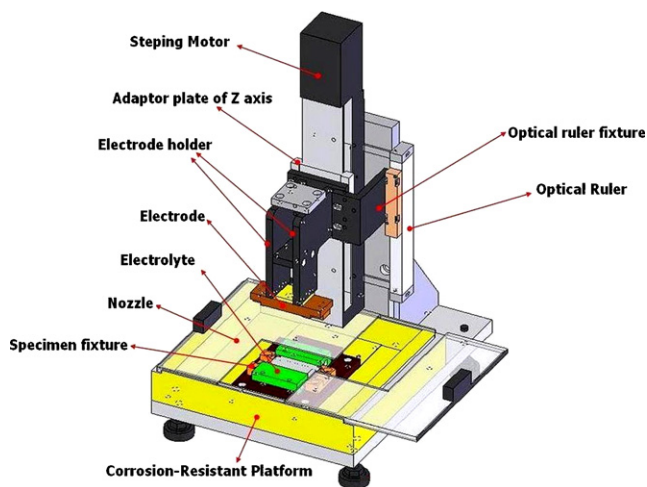


Fig. 1. Schematic plot of the EMM experimental setup.

2. Electrochemical micro-machining and research procedures

2.1. Electrochemical micro-machining

The EMM process is an anodic dissolution process. In general, the compositions of electrolyte are neutral salts. In this study, the 20 g L^{-1} of NaNO_3 solution had been used as the electrolyte. Fig. 1 shows the schematic plot of the EMM experimental setup.

During the EMM process, the metallic ions of the anodic dissolution will migrate toward the cathode. When metallic ions reacted with the OH^- , it will form the metallic hydride and oxide. At the same time oxygen is generated on the anode while hydrogen is generated on the cathode. Theoretically, only water was consumed in the process.

The accuracy of the EMM fabrication could be greatly influenced by several factors such as the uniformity of electric field between two electrodes, the flow rate of electrolyte, and the metallic reactant or the oxide concentration etc. One of the major factors is the amount of metallic reactant or the oxide. From the literatures [9] showed the reactant may accumulate or deposit on the electrode surface especially on the anode surface. The refreshing of the electrolyte and the continuity of the EMM process could be hampered by the high concentration of reactants on the anode surface resulting unstable operation voltage or current. The overcutting or undesirable shape of the anode may be fabricated.

2.2. Research procedures

In this paper, thin metallic bipolar plates produced by the EMM fabrication process were assembled into a single cell for testing. The 2D forming multiphysics model was simulated using the commercial software, COMSOL version 3.2. The bipolar plate material was SUS 304 stainless steel measuring $4 \text{ cm} \times 4 \text{ cm} \times 0.6 \text{ cm}$. The reactive area was $2 \text{ cm} \times 2 \text{ cm}$. The shape of the cathode tool was the inverse shape of the flow channel with rectangular and smooth surface. Each rectangular slots was $300 \mu\text{m}$ (width) \times $300 \mu\text{m}$ (height) \times 20 mm (length).

The design variables for both the simulation and the experiments were the operating potential, pulse rate and the inter-electrode gap (IEG) value. Duty cycle and processing time remained constant. In addition, the material removal rate of the flow channel EMM process was one of the key issues of fabrication accuracy. However, this depends on the reactant concentration in the IEG. Thus, the reactant concentration in the IEG was employed to eval-

uate the parametric effects on the fabrication accuracy. From the results of the simulation, the correct experimental variables were chosen to conduct the EMM process. After the process, the profile of the flow channel was measured by means of a 3D laser scanning microscope of VK-9700 of Keyence Inc.

2.3. Model assumptions

The electrochemical micro-machining is an anodic dissolution process under the electrochemical reaction. The metallic reactants (i.e. metallic hydride and metallic oxide) may accumulate on the electrode. Therefore, the refreshing of the electrolyte and continuity of the EMM process could be affected by these reactants. It had become one of the key factors in influencing the accuracy of anode shape fabrication. In addition, according to the Faraday's law, the metallic ions of the anodic dissolution are proportional to the applied current in the EMM process. Therefore, the goal of this study was to find out the effects of the pulse current parameters on the surface reactants concentration distribution. The numerical model was established to simulate the variation of reactant concentration under different pulse current conditions. In order to simply the model and to compare with the single channel experiment, the major assumptions of the model were,

- (1) The species of the EMM process are the metallic ions of anodic dissolution under the electrochemical reaction.
- (2) The EMM process is ideal. All of the reactants (i.e. metallic hydride and oxide) were formed by all of the metallic ions of the anodic dissolution. The amount of ions, once the process started, is equal to the charge of the given current as represents in i .
- (3) The diffusion coefficient ($1.0\text{E}-6 \text{ cm}^2 \text{ s}^{-1}$) and conductivity coefficient (1.542 S) of the diluted electrolyte were fixed, remain constant and measured by experiments.
- (4) The electrolyte is stationary in the single channel fabrication experiments. Therefore, flow velocity of electrolyte was assumed zero in the numerical model. The transport process of the reactant was enabled only by diffusion.
- (5) The model was isothermal.
- (6) To be consistent with experimental conditions, the equal on and off pulse periods was used in the model.

2.4. Numerical simulation models

Multiphysics models for current distribution and diffusion were established using COMSOL commercial software. The design variables were pulse rate, operating potential and IEG value. The pulse current was governed by the function "f1ch1s" of the COMSOL software. It was employed to establish the pulse function. The wave of this pulse function was base on sine wave. The pulse rate and duty cycle are also included. The fixed variables were composition of the electrolyte, concentration of the electrolyte and the duty cycle.

A smaller IEG may provide better fabrication precision, because there was a more concentrated electrical field between the two electrodes. However, it might also result in non-uniform and/or insufficient flow of the electrolyte, causing non-uniform metal removal [10]. Therefore, the IEG value was set at $200 \mu\text{m}$ and $300 \mu\text{m}$, respectively.

In order to improve the fabrication accuracy of the EMM process, especially for micro-scale fabricating, the operating potential and the electrolytic concentration should be small. For example, Bhattacharyya et al. [8] proposed an EMM fabrication method. The fabrication processes used a cathode electrode shaped like a milling tool incorporated in the NC machining path. His results showed that with a lower operating potential, sufficient electrolytic concentration and high pulse rate the amount of micro-sparking and the

Table 1
Boundary conditions of the numerical models.

Boundary settings of the current distribution model				
Boundary no.	1, 8	2	3, 4, 6, 7	5
Boundary cond.	Electric insulation	Electric potential	Electric insulation	Ground
Setting	$n \cdot j = 0$	$V = V_0$	$n \cdot j = 0$	$V = 0$
Boundary settings of the diffusion model				
Boundary no.	5	1, 8	2, 3, 4, 6, 7	
Boundary cond.	Conct.	Flux	Insulation	
Setting	$C = C_0$	Flux = 0	$n(-D \nabla C) = 0$	

control of metal removal can be improved. The operating potential was between 6 V and 10 V and the electrolyte concentration was below 20 g L⁻¹. Therefore, two levels of operating potential (V_0), 5 V and 7 V, and 20 g L⁻¹ of electrolytic concentration of NaNO₃, were used in our study. The coefficient of diffusion obtained from the diffusion tests is 1.0E-6 cm² s⁻¹. Four levels of pulse rates, 15 ms, 30 ms, 60 ms, and 100 ms were tested in order to investigate the effect of the pulse rate on the EMM process.

The cathode was stationary during the simulation and during EMM fabrication. In order to simplify the numerical simulation, a 2D model was assumed. The geometry of the numerical simulation was shown in Fig. 2.

The current density between two electrodes is based on Faraday’s law. It could be stated as the sum of the mobile ions of all species, as shown in Eq. (1).

$$I = -F \sum z_i N_i \quad (1)$$

In addition, the typical electrolytic composition of the ECM or EMM process consists of neutral salts such as NaCl and NaNO₃, and the electron charge in the electrolyte of the simulation model was also assumed to be neutral as shown in above assumption (2). Therefore, the number of electrons of the species is zero ($z_i N_i = 0$). The equation is transformed into Eq. (2).

$$I = -F \sum -z_i^2 u_i F C_i \nabla \phi \quad (2)$$

where I is the current density, Z_i denotes the number of electrons of species i , N_i is the transport vector of species i , and F is Faraday’s constant, u_i is the coefficient of mobility of species i , $\nabla \phi$ is the gradient of the electrical field, and C_i denotes the concentration of species i .

By reformulating Eq. (2) into Ohm’s law, the governing equation of the current distribution can be shown as Eq. (3).

$$I = -\sigma \nabla \phi \quad (3)$$

where ϕ is the electrical field, and σ is the coefficient of conductivity.

For the diffusion phenomena, the governing equation is based on Fick’s law, as shown in Eq. (4). From the computed results of Eq. (3), the Heaviside function of the current distribution can be computed

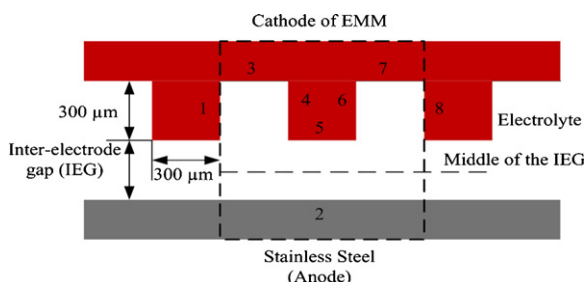


Fig. 2. Specifications of the numerical model.

Table 2
Parameters and coefficients of the model.

Operation voltage (Φ)	5 V	7 V		
Pulse rate	15 ms	30 ms	60 ms	100 ms
IEG value	200 μm	300 μm		
Electrolyte conductivity (σ)	1.542 S			
Diffusion coefficient (D)	1E-6 cm ² s ⁻¹			
Electrolyte flow	Stationary			

and set as the reactant concentration in the diffusion model.

$$\frac{\partial C}{\partial t} + \nabla(-D \nabla C + Cu) = 0 \quad (4)$$

where C is the concentration of diffusive species, and D is the coefficient of diffusion.

2.5. Parametric settings and boundary conditions

All the boundaries in the current distribution model are dielectric except for the two surfaces of the anode and the cathode facing each other, the conditions of which are set at $V = 0$ and $V = V_0$. In the diffusion model, the reactant formed on the anode will be diffused toward the cathode. Hence, the Heaviside function of the current distribution is set up as the initial concentration on the anode surface, boundary no. 5. Boundary nos. 1 and 8 were set as flux = 0. Boundary nos. 2–4, 6, 7 are set as insulation. These boundary conditions are listed in Table 1. The overall modeling parameters are listed in Table 2. The experimental parameters are listed in Table 3.

3. Results and discussions

3.1. Simulation results

The trends of the reactant concentration in the electrode gap are similar between the operating potentials of 5 V and 7 V. The results of the operating potential of 7 V are discussed here. Figs. 3–6 show the results of the envelopes of the reactant concentration in the IEG under different pulse rates.

Figs. 3 and 5 show that the peak values of the reactant concentration are 1.2E5 and 3.4E4. These results show that larger IEG values have smaller concentration values. Regardless of the IEG value, the variation in concentration stabilizes when the value of the concentration decreases to 50% of peak value. Based on the above analyses, regardless of the electrode gap values, the reactant can be flushed effectively from the IEG with a faster pulse rate of 15 ms and 30 ms, respectively. However, the same phenomena could not be observed

Table 3
Parameters setting of the experiments.

Operation voltage (Φ)	7 V
Pulse rate	33.3 ms
Electrolyte	NaNO ₃
Concentration	20 g L ⁻¹
Electrolyte flow	Stationary
IEG value	200 μm
Process time	10 min

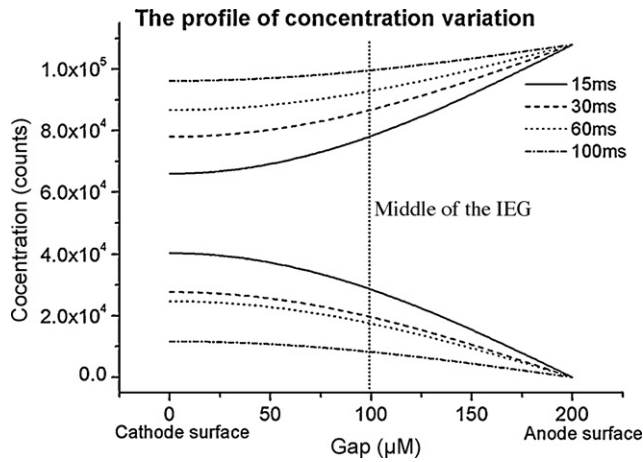


Fig. 3. The envelopes of reactant concentration under different pulse rate (IEG value = 200 μm).

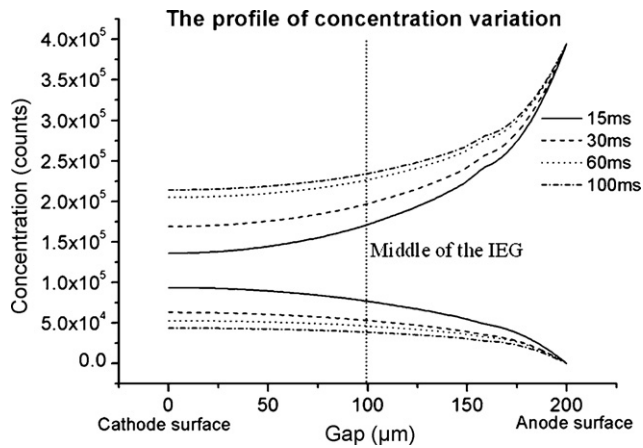


Fig. 4. The envelopes of reactant concentration at the edge under different pulse rates (IEG value = 200 μm).

with slower pulse rates such as 60 ms and 100 ms. This may be due to the fact that the reactant may be difficult to refresh by diffusion during the time-off period. Therefore, the pulse rate is the key factor for the reactant flushing.

The results of the IEG value at 200 μm , were selected to demonstrate the effects of pulse rate. Fig. 3 shows that the reactant concentration diffuses effectively from the anode and decreases

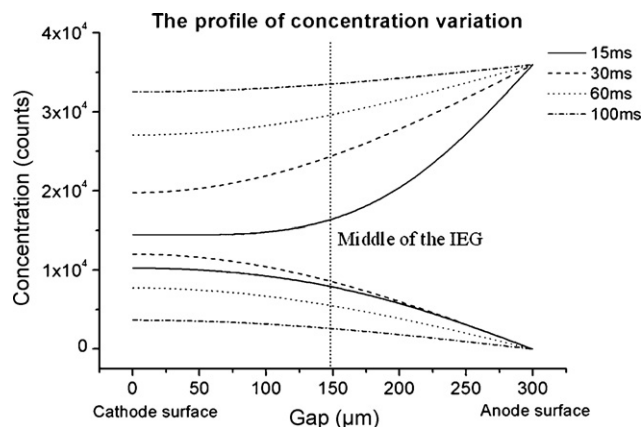


Fig. 5. The envelopes of reactant concentration under different pulse rates (IEG value = 300 μm).

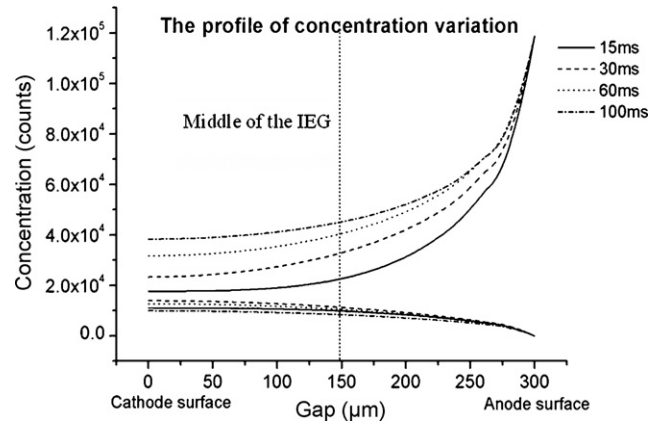


Fig. 6. The envelopes of reactant concentration at the edge under different pulse rates (IEG value = 300 μm).

to 50% at the middle of the IEG, IEG value = 100 μm , with a pulse rate of 15 ms. At the middle of the IEG, the low and high values of the reactant concentration are $3.2\text{E}4$ and $7.0\text{E}4$, respectively. The difference is 218%, showing that the refreshing of the electrolyte is efficient and stable, resulting in a stable electrochemical process. As the pulse rate reduces to 30 ms, the diffusion rate slows down and reduces only 20% at the middle of the IEG where the low and high values of the reactant concentration are $1.4\text{E}4$ and $9.0\text{E}4$, respectively. The difference is now 643%. Hence, the uniformity and the stability of the electrolyte have degraded with the decrease in pulse rate.

As shown in Fig. 3, when the pulse rate decreases to 60 ms, the polishing time in each duty cycle becomes longer, the diffusion rate becomes even slower and the reactant starts to accumulate. At the middle of the IEG, the reactant concentration decreases by only 2%. The reactant may have difficulty in refreshing by diffusion during the time-off period. This will increase the electrical resistance and decrease the process effectiveness. When the pulse rate decreases to 100 ms, the diffusion mechanism is completely ineffective during the time-off period.

It is evident from the above results that a faster pulse rate promotes a uniform and fresh reactant concentration, provides stable process conditions, and results in a better metal removal rate and a higher level of fabrication accuracy.

Similar to Fig. 3, the reactant concentration in Fig. 4 decreases by 50% in the middle of the IEG at the edge with a pulse rate of 15 ms. The low and high values are $5.4\text{E}4$ and $1.5\text{E}5$, respectively. The difference is 64%. This indicates that the extra electrons resulting from the terminal effect will not accumulate in the IEG at the edge. As the pulse rate decreases to 30 ms, the reactant concentration decreases by 45% in the middle of the IEG at the edge. The low and high values are $5.0\text{E}4$ and $1.625\text{E}5$, and the difference is 69%. As the pulse rate further decreases to 60 ms, the respective values are $4.0\text{E}4$, $1.7\text{E}5$ and the difference is 76%.

Therefore, it can be concluded that the effects of the terminal effect are not sensitive to the pulse rate. The refreshing of the electrolyte in the IEG at the edge is effective. The over-cut in the horizontal direction will be suppressed resulting in a more precise (vertical) processed profile of the anode (workpiece). Thus, a higher level of fabrication accuracy can be achieved.

3.2. Experiments and verification

3.2.1. Single channel experiments

From the above numerical simulation results, the process parameters of a 33.3 pulse per s, 7V operating potential, 200 μm gap value and 20g L^{-1} electrolyte concentration are selected for

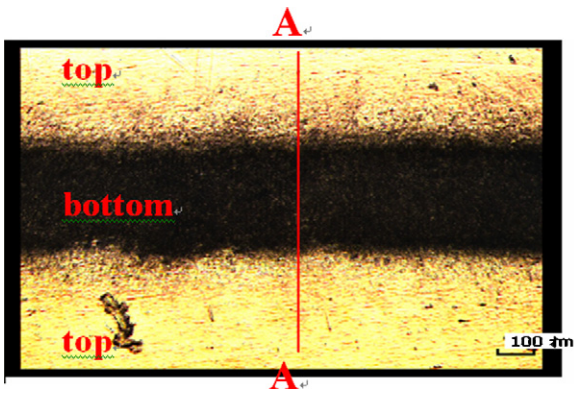


Fig. 7. OM. Picture of EMM processed specimen without pulse rate.

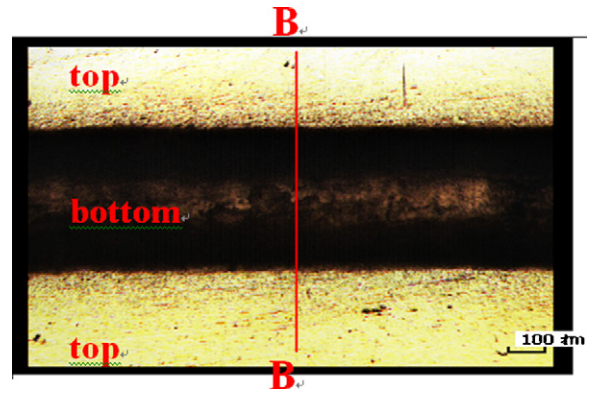


Fig. 8. OM. Picture of EMM processed specimen with pulse.

performing the single channel EMM fabrication experiments. The processing time is 10 min. Both the experiments for the DC current and the pulse current were conducted in order to evaluate the effects of the pulse rate. The percentage of over-cut, the depth of the single channel and the profile of the processed channel are indices of the fabrication precision, the efficiency of metal removal and the precision of the dimensions. A rectangular cathode measuring 300 μm wide × 300 μm high × 20 mm long was manufactured by UV-LIGA and the electroforming process [11]. It was insulated with parylene on the side wall [12]. The anode is a 40 mm² × 1 mm thick sheet of 304 stainless steel.

Figs. 7 and 8 show pictures taken by an optical microscope of a specimen processed by DC and pulse current. Fig. 9 is the 2D sectional profile of Figs. 7 and 8. Comparing a specimen processed by EMM with DC and pulse current, Fig. 9 shows that the single channel width on the top is 480 μm while it is 218 μm at the bottom. The depth of the single channel is 45 μm. The ratio of the width on the top to the width at the bottom is 220%. The ratio of overcutting is 120%. The overcutting of the single channel on

the side wall is severe and obvious. On the other hand, the specimen width with pulse current is 450 μm on the top and 340 μm at the bottom. The depth of the single channel is 65 μm. The ratio of the width on the top to the width at the bottom is reduced to 132%. The ratio of overcutting is 32%. Therefore, the shape of the single channel is sharper and better defined, and the depth of the single channel is deeper with the pulse current. This verifies that the pulse current improves the refreshing of the electrolyte as well as the stability of the reactant concentration. As a result, the metal removal rate is greatly improved, and the ratio of overcutting is reduced from 120% to 32%. It is evident from the numerical simulation results that the pulse current restrains the terminal effect.

3.2.2. Flow channels in the bipolar plate fabrication process

The operating conditions of the flow channels or flow field in the bipolar plate EMM fabrication process are taken to be the same as the simulation results of the single channel forming process. The flow-field channels are fabricated in less than 5 min. The electrode

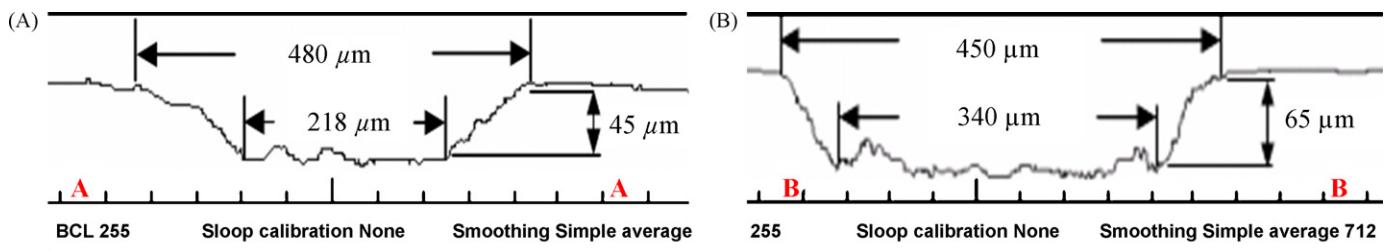


Fig. 9. Profile of the single channel processed by the EMM fabrication process. (a) Without pulse current control. (b) With pulse current control.

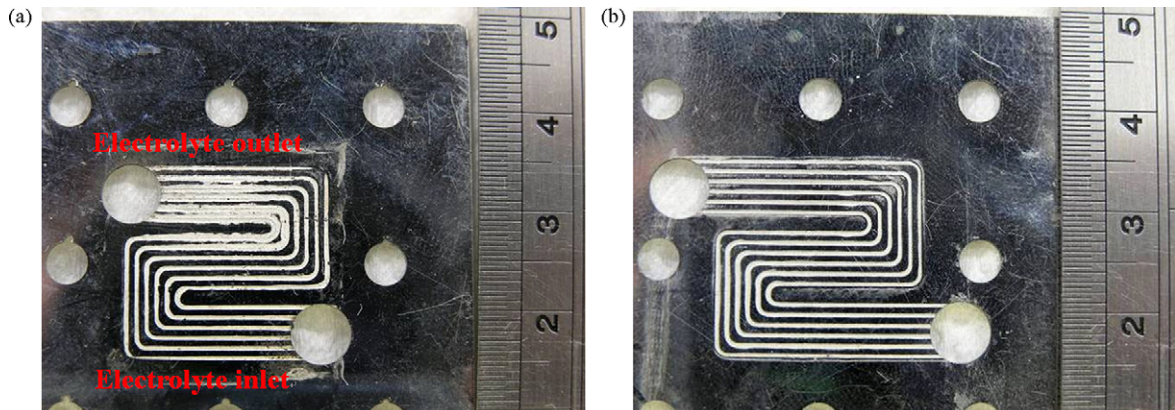


Fig. 10. The surface image of the bipolar plate fabricated by the EMM process. (a) Without pulse current control. (b) With pulse current control.

has serpentine shape, and is made of brass with insulated side walls with parylene.

Fig. 10 shows the finished part of the SS304 bipolar plates with and without pulse current control. Regardless of DC or pulse current control, at the electrolyte inlet area, the forming process can provide a uniform and accuracy flow channel surface. However, from the profile measurement of the surface geometry it is evident that the flow channels using pulse current control in the EMM fabrication process are sharper and deeper. Near the electrolyte outlet, the geometry of the flow channels created without pulse current control are not as good as those with pulse current control, and their depth and width are not uniform. The over-cut of the width is substantial and the depth is insufficient. This is due to the fact that at the inlet location the electrolyte is freshest and most rapid, and thus the dimensions of the flow channels are more accurate there. Near the outlet section, the electrolyte goes through several up and down turns along the flow channel pattern and becomes more turbulent and non-uniform. In addition, the DC current cannot provide the necessary pulse-off time during the fabrication process, and as a result the refreshing of the electrolyte at the outlet is insufficient. On the other hand, the shape of the flow channels with pulse current control is more uniform and defined. The results show that the pulse current improves the refreshing of the electrolyte as well as the stability of the reactant concentration. Therefore, the metal removal rate and the flow channel geometry of the bipolar plate are both greatly improved, producing a uniform channel.

4. Conclusions

1. Current distribution and diffusion models were established for the flow channel of the bipolar plate EMM fabrication process. The simulation results showed the effectiveness of a pulse current on the terminal effect. This was verified by the EMM experiments and the profile measurements of the processed flow channel.
2. Based on the simulation results, and regardless of the IEG values, the reactant can be flushed effectively from the electrode gap value with a faster pulse rate.
3. The simulation results showed that a pulse rate of say less than 20–30 ms can greatly improve the stability of the process conditions. A shorter pulse rate may improve the process conditions and their uniformity even further.
4. The pulse current increases the metal removal rate by 50% and reduces the ratio of the width on the top and at the bottom by a factor of 4, which substantially improves the fabrication accuracy. It is also consistent with the numerical simulation.
5. The effect of the pulse rate reduces the effect of the terminal effect resulting in an improved over-cut control and a higher fabrication accuracy.

Acknowledgments

This work was accomplished with the much appreciated financial support from the “Aim for the Top University” project of the Ministry of Education of Taiwan, ROC and the Yuan Ze Fuel Cell Centre.

References

- [1] H. Wang, J.A. Turner, *J. Power Sources* 128 (2004) 193–200.
- [2] Y. Hung, K.M. El-Khatib, H. Tawfik, *J. Power Sources* 163 (2006) 509–513.
- [3] D.R. Hodgson, B. May, P.L. Adcock, D.P. Davis, *J. Power Sources* 96 (2001) 233–235.
- [4] M. Ghaemi, L. Binder, *J. Power Sources* 111 (2002) 248–254.
- [5] B. Bhattacharyya, J. Munda, *Int. J. Mach. Tools Manuf.* 43 (2003) 1301–1310.
- [6] M. Kock, V. Kirchner, R. Schuster, *Electrochim. Acta* 48 (2003) 3213–3219.
- [7] C. Rosenkranz, M.M. Lohrengel, J.W. Schultze, *Electrochim. Acta* 50 (2005) 2009–2016.
- [8] B. Bhattacharyya, M. Malapati, J. Munda, *J. Mater. Process. Technol.* 169 (2005) 485–492.
- [9] D. Landolt, P.F. Chauvy, O. Zinger, *Electrochim. Acta* 48 (2003) 3185–3201.
- [10] A.K.M.D. Silva, J.A. McGeough, *J. Mater. Process. Technol.* 76 (1998) 165–169.
- [11] W. Ehrfeld, *Electrochim. Acta* 48 (2003) 2857–2868.
- [12] H. Hocheng, Y.H. Sun, S.C. Lin, P.S. Kao, *J. Mater. Process. Technol.* 140 (2003) 264–268.